



## Upconversion emission from amorphous $\text{Y}_2\text{O}_3:\text{Tm}^{3+}, \text{Yb}^{3+}$ prepared by nanosecond pulsed laser irradiation

C.B. Zheng<sup>a,b</sup>, Y.Q. Xia<sup>c</sup>, F. Qin<sup>a,b</sup>, Y. Yu<sup>a,b</sup>, J.P. Miao<sup>a</sup>, Z.G. Zhang<sup>a,b,\*</sup>, W.W. Cao<sup>a,b,d,\*</sup>

<sup>a</sup> Department of Physics, Harbin Institute of Technology, 150001 Harbin, PR China

<sup>b</sup> Laboratory of Sono- & Photo-Theranostic Technologies, Harbin Institute of Technology, 150001 Harbin, PR China

<sup>c</sup> National Key Lab of Tunable Laser Technology, Harbin Institute of Technology, 150001 Harbin, PR China

<sup>d</sup> Materials Research Institute, The Pennsylvania State University, University Park, 16802 PA, United States

### ARTICLE INFO

#### Article history:

Received 22 January 2011

In final form 27 April 2011

Available online 30 April 2011

### ABSTRACT

$\text{Y}_2\text{O}_3:\text{Tm}^{3+}, \text{Yb}^{3+}$  was prepared by nanosecond pulsed laser irradiation. The X-ray diffraction pattern shows that the material produced by laser irradiation is amorphous, which presents strong blue upconversion emission under the excitation of 976 nm diode laser. The relative intensity of the blue emission to the infrared one is linearly dependent on the pump power and is an order of magnitude higher than that of the bulk material. The analyses of rate equations and the time-resolved spectroscopic results indicate that the enhancement of the blue upconversion is attributed to the longer lifetime of the levels of the  $\text{Tm}^{3+}$  and  $\text{Yb}^{3+}$  ions.

© 2011 Elsevier B.V. All rights reserved.

### 1. Introduction

In the recent years, upconversion (UC) emissions from rare earth doped materials have gained much attention due to many potential applications, such as all-solid state lasers [1,2], three-dimensional displays [3], biological labeling [4–6], and luminescent switchers [7]. Excitation is easily achieved by a commercially available continuous wave (CW) infrared diode laser, which is compact, power-rich, and inexpensive. For technological applications and basic research, studies on the dependence of UC property on different host matrices and synthesis methods are very important, which can help the realization of controllable UC emissions, enhancing the quantum yield of the luminescence, and understanding the UC dynamics.

The local environment around the active ions and the chemical components in a host material greatly affect the UC efficiency and emission spectra. Qin et al. reported enhancement of ultraviolet UC in  $\text{Yb}^{3+}$  and  $\text{Tm}^{3+}$  codoped fluoride film due to the decrease of Judd–Ofelt parameter  $\Omega_2$ , which is related to the symmetry of the ligand field [8]. Qi et al. indicated that the change of local structure around the active ions lead to new emission peaks and the red shift of the charge-transfer band of the  $\text{Eu}^{3+}$  ions [9]. Patra et al. investigated the effect of crystal size and crystal phase on UC luminescence in  $\text{ZrO}_2:\text{Er}^{3+}$  nanocrystals [10]. In relevant literatures, the UC samples were synthesized by chemical methods, such as sol-

gel [10,11], coprecipitation [12], solution combustion [13,14], and controlled hydrolysis synthesis procedures [14]. In these chemical methods, the contamination caused by chemical precursors or additives may lead to the change of the UC dynamics and affect the UC luminescence results, especially in the nanomaterials [12,13].

In a recent work, ultrafine  $\text{Y}_2\text{O}_3:\text{Pr}^{3+}, \text{Yb}^{3+}$  nanoparticles were prepared by femtosecond pulsed laser irradiation [15]. Because the method can avoid possible chemical contamination, these nanoparticles showed higher UC efficiency, compared with nanoparticles synthesized by typical sol-gel method. However, the amount of the product is very small in the synthesis by femtosecond pulsed laser ablation. Different from the above method, nanosecond pulsed laser was used to treat sample surface, which produced a process of melting and resolidification. Larger amount of materials can be obtained [16].

Based on the above consideration, the main goal of this work is to investigate the structural properties and UC emissions of  $\text{Y}_2\text{O}_3:\text{Tm}^{3+}, \text{Yb}^{3+}$  prepared by the nanosecond pulsed laser irradiation. The structural properties of the product were analyzed by the grazing incidence X-ray diffraction and field emission scanning electron microscopy. The pump power dependence of the UC emission spectra and the intensities of blue to infrared band were measured. These spectra behaviors were explained by the rate equations and time-resolved spectroscopy.

### 2. Experiments

The preparation procedure is similar with that employed in previously [17,18]. The stoichiometric mixture of  $\text{Y}_2\text{O}_3$ ,  $\text{Tm}_2\text{O}_3$  and

\* Corresponding authors at: Department of Physics, Harbin Institute of Technology, 150001 Harbin, PR China. Fax: +86 45186412828 (Z.G. Zhang), +1 8148652326 (W.W. Cao).

E-mail addresses: [zhangzhiguo@hit.edu.cn](mailto:zhangzhiguo@hit.edu.cn) (Z.G. Zhang), [cao@math.psu.edu](mailto:cao@math.psu.edu) (W.W. Cao).

$\text{Yb}_2\text{O}_3$  powders is pressed into a round disk with 13 mm diameter and 2 mm in thickness. The molar ratio of  $\text{Y}_2\text{O}_3$ ,  $\text{Tm}_2\text{O}_3$  and  $\text{Yb}_2\text{O}_3$  were fixed at 100:0.5:3.5. The target was fixed on a two-dimensional translational platform which was controlled by a computer. The laser beam was focused using a 10-cm-focal-length lens onto the solid target. The laser beam scanned the whole surface of the sample with a track of square-wave lines by controlling the two-dimensional translational platform. The solid target moved at a speed of 1 mm/s during the experiments and the distance between parallel lines is 0.2 mm. The laser source employed was a 532 nm Nd: YAG nanosecond laser (Spectra Physics) with a pulse width of 10 ns operated at a repetition rate of 10 Hz. The pulse energy was 400 mJ, and the laser intensity is estimated to be  $5.1 \times 10^8 \text{ W/cm}^2$ . The surface of the irradiate target was investigated for the structure and optical properties, but no special treatment was performed.

For comparison, bulk material with the same composition was prepared using the sol-gel method followed by high temperature annealing. The synthesis routine is described below: The mixtures mentioned above were dissolved in dilute nitric acid by stirring at 80 °C. Then, citric acid was added into the solution with a mole ratio of cation to citric acid of 1:4. The pH of the solution was adjusted to 6.0 by the addition of ammonium hydroxide. The solution was dried at 120 °C for 12 h. The resulting black mixture was sintered at 800 °C for 2 h. The powders obtain were pressed into a round disk, which were sintered again at 1300 °C for 20 h. This sample is referred as HT sample and the sample prepared by the laser irradiation is referred as LI sample in the following text. According to the FT-IR absorption spectra, the influence of the groups with large phonon mode could be ignored in both samples.

Grazing incidence X-ray diffraction (GIXRD) was used to determine the crystalline phases of the samples. The GIXRD device employed were a Philips X-ray diffractometer (XRD) with  $\text{Cu K}\alpha$  radiation. During the diffraction experiment, the incidence angle was fixed at 1°. The morphology of the product was characterized by field emission scanning electron microscopy (SEM, Hitachi S-4800). The room temperature UC emissions were recorded using a monochromator (Zolix Instruments Co. Ltd., Beijing) and a photomultiplier tube (Hamamatsu CR131) under the excitation of 976 nm diode laser. The light beam was focused to an area of 2 mm<sup>2</sup>. The fluorescence lifetimes were measured by a digital storage oscilloscope (Tektronix 5052).

### 3. Result and discussion

The normal-incidence XRD patterns of both samples show identical phase, which is consistent with the cubic phase of yttrium oxide (referenced JCPDS 86-1107). However, no valuable information was obtained. Hence, the grazing XRD experiments were conducted. Figure 1a shows the GIXRD patterns for both samples. From Figure 1a one can see that the amorphous structure produced by the pulsed laser is only on the surface. The weak diffraction peaks at 29° and 49° probably come from raw material at the side face of the disk or under the top layer. While, the HT sample exhibits pure cubic structure. Figure 1b shows the SEM micrograph of the LI sample. It can be observed that the surface of the sample demonstrated a typical morphology resulted from surface melting and subsequent fast recrystallization of the liquid phase after high energy laser irradiation.

Figure 2 shows the UC spectra of the LI sample (a) and HT sample (b) under the excitation of 390 mW, 976 nm diode laser. These UC emissions all have two emission bands centered at 490 and 810 nm, respectively. The spectra were normalized to the intensity at 486 nm for easy comparison. Interestingly, the relative intensity of the blue band to the near infrared band is obviously different for

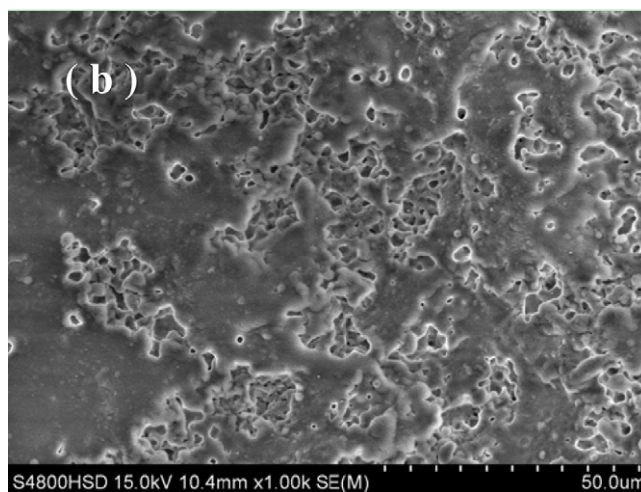
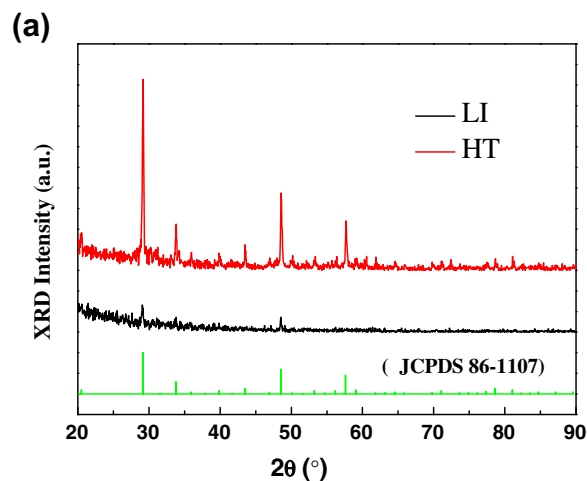


**Figure 1.** (a) GIXRD pattern of  $\text{Y}_2\text{O}_3:\text{Tm}^{3+}, \text{Yb}^{3+}$  produced by nanosecond pulse laser irradiation and corresponding bulk material with angle of X-ray incidence 1°; (b) SEM image of the sample produced by nanosecond pulse laser irradiation.

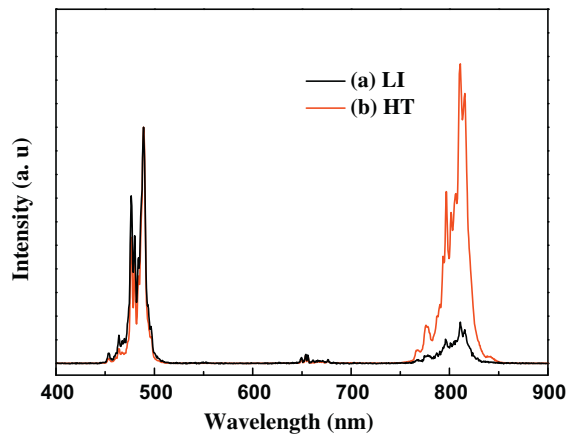


**Figure 2.** UC spectra of  $\text{Y}_2\text{O}_3:\text{Tm}^{3+}, \text{Yb}^{3+}$  produced by nanosecond pulse laser ablation (a) and bulk material (b) excited by 976 nm DL at 390 mW.

samples synthesized by different methods. In the HT material, the emission at 810 nm is much stronger than the one at 490 nm. While in the LI sample, the emission centered at 490 nm is dominant in the spectrum. The strong blue emission is propitious to the potential application of blue UC laser [1]. The relative intensity

of 490 nm/810 nm emitted intensity as a function of the excitation power is shown in Figure 3. It can be seen that the relative intensity is increased linearly with the excitation power for both samples within the excitation range (50–390 mW). The slopes are  $3.85 \times 10^{-3}$  for the LI sample and  $3.60 \times 10^{-4}$  for the HT sample. And the relative intensity of the LI sample is always ten times as high as that of the HT sample.

To investigate this discrepancy in the spectra, the upconversion mechanism of  $\text{Y}_2\text{O}_3:\text{Yb}^{3+}, \text{Tm}^{3+}$  under the 976 nm excitation were further studied. The emissions of 480 and 810 nm are assigned to the transition from  $^1\text{G}_4$  to  $^3\text{H}_6$  and  $^3\text{H}_4$  to  $^3\text{H}_6$ , respectively. The dependence of UC intensities on the pump power was measured and given in Figure 4 in double-logarithmic representation. For an unsaturated UC process, the number of photons, which are required to populate the upper emitting state, can be obtained by the following relation [19],

$$I \propto P^n,$$

where  $I$  is the fluorescence intensity,  $P$  is the pump laser power, and  $n$  is the number of the laser photons required. It was observed that power dependence slopes are 2.40 and 1.57 for the 490 and 810 nm UC emissions, respectively, in the LI sample, and the slopes are 2.74 and 1.87 for the two corresponding emissions in the HT sample. This indicates that three or two photons are required to populate the  $^1\text{G}_4$  and  $^3\text{H}_4$  level, respectively. Due to the mismatch of the energy level gap of  $\text{Tm}^{3+}$  ion and the pump photon, the  $^1\text{G}_4$  level is populated by three step energy transfer while the  $^3\text{H}_4$  level is populated by two step energy transfer from the  $\text{Yb}^{3+}$  ions to the  $\text{Tm}^{3+}$  ion, as illustrated in the simplified energy level diagram in Figure 5 [7,20]. Briefly, the  $\text{Yb}^{3+}$  ions are excited by 976 nm photons and transit from the ground state  $^2\text{F}_{7/2}$  to  $^2\text{F}_{5/2}$ . Then, three excited  $\text{Yb}^{3+}$  ions subsequently transfer their energies to  $\text{Tm}^{3+}$  ions and make them transit from  $^3\text{H}_6$  to  $^3\text{H}_5$ , from  $^3\text{F}_4$  to  $^3\text{F}_{2,3}$  and from  $^3\text{H}_4$  to  $^1\text{G}_4$  assisted by multi-phonon nonradiative relaxation. The  $\text{Tm}^{3+}$  ions in  $^1\text{G}_4$  state emit photons near 480 nm and return to the  $^3\text{H}_6$  state. A fraction of  $\text{Tm}^{3+}$  ions in  $^3\text{H}_4$  state transit to the ground state and emit photons near 810 nm.

In fact, the  $n$  is usually smaller than the theoretical integer value because the competition between the linear decay and the upconversion for the depletion of intermediate excited states [19]. Under the excitation of low pump power, linear decay is dominant and the  $n$  value would be close to an integer. However, as the pump power increases, upconversion becomes dominant and the  $n$  value would be smaller and even approaches 1, where a ‘saturation’ of the emission intensity would be observed. Based on the observed

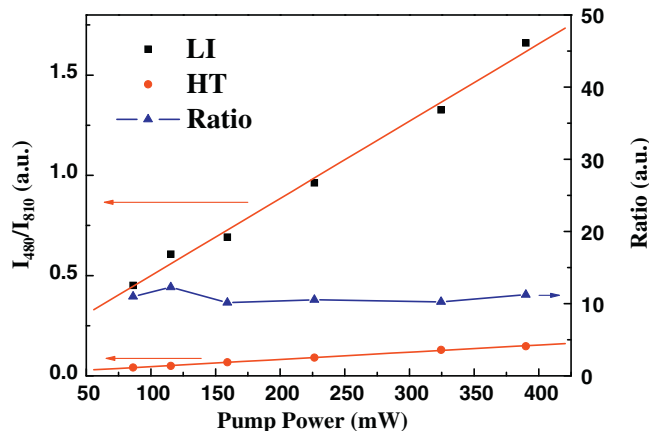


Figure 3. Pump power dependence of the relative intensity of 490 nm/810 nm emissions from samples prepared by laser irradiation (LI) and bulk material (HT), and the ratio of the relative intensity in the LI sample to that of the HT sample.

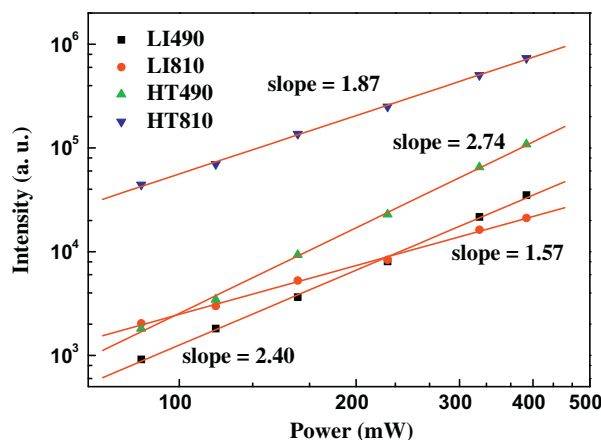


Figure 4. Pump power dependence of the UC emission intensity at 490 and 810 nm for both samples.

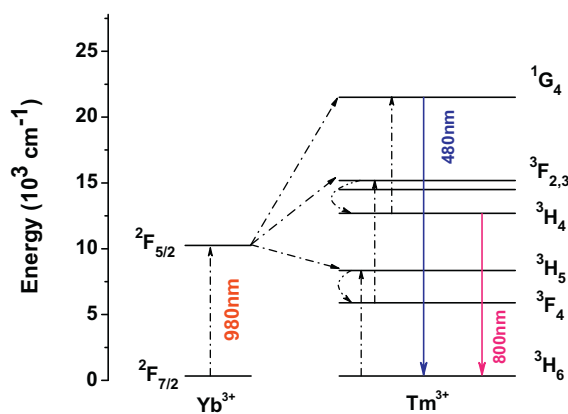


Figure 5. Energy level diagram of  $\text{Yb}^{3+}$  and  $\text{Tm}^{3+}$  ions in  $\text{Y}_2\text{O}_3$ .

$n$ -values, we can conclude that the upconversion process is more efficient in the LI sample.

We may use the following steady-state rate equations to further analyze the UC properties:

$$\frac{dn_{Y1}}{dt} = \sigma \rho n_{Y0} - n_{Y1} A_{Y1} - C_0 n_0 n_{Y1} = 0, \quad (1)$$

$$\frac{dn_1}{dt} = C_0 n_0 n_{Y1} - n_1 A_1 - C_1 n_{Y1} n_1 = 0, \quad (2)$$

$$\frac{dn_2}{dt} = C_1 n_1 n_{Y1} - n_2 A_2 - C_2 n_{Y1} n_2 = 0, \quad (3)$$

$$\frac{dn_3}{dt} = C_2 n_2 n_{Y1} - n_3 A_3 = 0, \quad (4)$$

where  $Y0$  stands for  $^2\text{F}_{7/2}$ ,  $Y1$  for  $^2\text{F}_{5/2}$ , 0 for  $^3\text{H}_6$ , 1 for  $^3\text{F}_4$ , 2 for  $^3\text{H}_4$ , and 3 for  $^1\text{G}_4$ ;  $n_i$ ,  $C_i$  are population density and coefficient of energy transfer, respectively, and  $\sigma$ ,  $\rho$  are the absorption cross-section and energy density of the pump light, respectively. Due to the quick non-radiation decays:  $^3\text{H}_5 \rightarrow ^3\text{F}_4$  and  $^3\text{F}_{2,3} \rightarrow ^3\text{H}_4$ , the equations corresponding to the  $^3\text{H}_5$  and  $^3\text{F}_{2,3}$  energy levels have been ignored. We also do not need to consider the direct transition from  $^2\text{F}_{5/2}$  of  $\text{Yb}^{3+}$  to the excited levels of  $\text{Tm}^{3+}$  because of the large mismatch of the energy levels. The emission intensity is proportional to the spontaneous emission, that is,

$$I_i \propto n_i A_i. \quad (5)$$

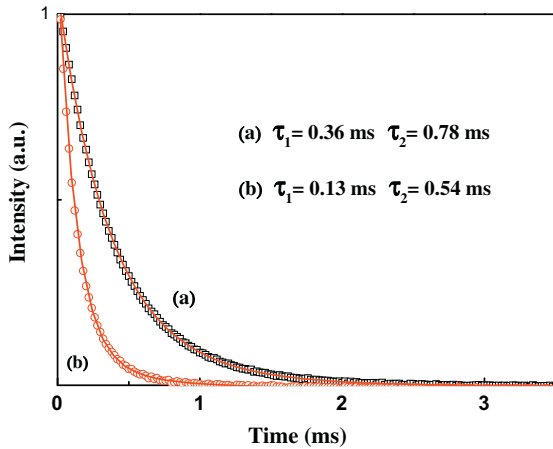


**Figure 6.** Decay profiles of the  $^1G_4 \rightarrow ^3H_4$  transition in  $Y_2O_3:Tm^{3+}, Yb^{3+}$  produced by laser irradiation (a) and bulk material (b).

From Eqs. (1)–(5), we can get the relative intensity of 490 nm/810 nm as follows:

$$R = \frac{I_1}{I_2} \propto \frac{n_3 A_3}{n_2 A_2} = \frac{C_2 n_{Y1} n_2}{C_1 n_{Y1} n_1 - C_2 n_{Y1} n_2} = \frac{C_2 \sigma \rho n_{Y0}}{A_2 (A_{Y1} + C_0 n_0)} \quad (6)$$

where  $R$  is the relative intensity. From Eq. (6) and  $A_2 = \frac{1}{\tau_2}$ , where  $\tau_2$  is the lifetime of the  $^3H_4$  level, one can conclude that the relative intensity is proportional to the pump intensity and the lifetimes of the  $^3H_4$  level of  $Tm^{3+}$  and the  $^2F_5$  level of  $Yb^{3+}$ . The influence of the pump power is consistent with the results given in Figure 3.

To confirm the influence of the lifetimes of the energy levels, the decay time of 810 nm UC emission from both samples was measured and shown in Figure 6. All curves can be fitted very well by the double exponential decay function. We believe that the short lifetime is for the  $^3H_4$  level of  $Tm^{3+}$  and the long lifetime is for the  $^2F_5$  level of  $Yb^{3+}$ . These fitting results are summarized in Figure 6. Obviously, the lifetimes in the LI sample (0.36 and 0.78 ms) are longer than that of the HT sample (0.13 and 0.54 ms). It can be seen that the relative intensity increases with the corresponding lifetime, which is consistent with the conclusion of the rate equations. Therefore, the long lifetimes of the energy levels in the LI sample are responsible for the stronger blue UC emission.

The possible mechanism for the increase of the lifetimes of the energy levels in the LI sample is not fully understood. In the Letter of Guanshi Qin et al., the authors suggested that the UC emissions can be influenced by the change of the local host structure around the active ion by analyzing the Judd–Ofelt parameters [8]. Analogously, by the rate equations and the time-resolved experiment

results, we have demonstrated that the relative intensity of the blue UC emission to the infrared one is related to the lifetimes of the energy levels. The amorphous materials prepared by the laser irradiation present a relatively longer lifetimes of the energy levels. The long lifetimes are propitious to the UC processes of the higher energy levels, which lead to the higher relative intensity of the blue to the near infrared emissions.

#### 4. Conclusion

We have prepared  $Tm^{3+}, Yb^{3+}$  codoped  $Y_2O_3$  by nanosecond pulsed laser irradiation. The GIXRD pattern shows that the structure of the product on the sample surface is amorphous. The sample shows much improved upconversion properties compared with the bulk material. The relative intensity of the blue to the near infrared in the laser induced sample is ten times as high as that of the bulk material. Rate equation analyses and the lifetime measurements indicated that the laser irradiated samples have longer lifetimes of energy levels, which are in favor of the UC processes. Our results and analysis indicated that nanosecond pulsed laser irradiation is a good method to prepare more efficient UC materials.

#### References

- [1] S. Sanders, R.G. Waarts, D.G. Mehuys, D.F. Wetch, *Appl. Phys. Lett.* 67 (1995) 1815.
- [2] T. Sandrock, H. Scheife, E. Heumann, G. Huber, *Opt. Lett.* 22 (1997) 808.
- [3] E. Downing, L. Hesselink, J. Raltson, R. Macfarlane, *Science* 273 (1996) 1185.
- [4] G.S. Yi, H.C. Lu, S.Y. Zhao, G. Yue, W.J. Yang, D.P. Chen, L.H. Guo, *Nano Lett.* 4 (2004) 2191.
- [5] L.Y. Wang et al., *Angew. Chem. Int. Ed.* 44 (2005) 6054.
- [6] J.H. Zeng, J. Su, Z.H. Li, R.X. Yan, Y.D. Li, *Adv. Mater.* 17 (2005) 2119.
- [7] C. Jacinto, M.V.D. Vermelho, E.A. Gouveia, M.T. de Araujo, P.T. Udo, N.G.C. Astrath, M.L. Baesso, *Appl. Phys. Lett.* 91 (2007) 071102.
- [8] G.S. Qin et al., *J. Appl. Phys.* 93 (2003) 4328.
- [9] Z.M. Qi, C.S. Shi, W.W. Zhang, W.P. Zhang, T.D. Hu, *Appl. Phys. Lett.* 81 (2002) 2857.
- [10] A. Patra, C.S. Friend, R. Kapoor, P.N. Prasad, *Appl. Phys. Lett.* 83 (2003) 284.
- [11] E. De la Rosa, P. Salas, H. Desirena, C. Angeles, R.A. Rodríguez, *Appl. Phys. Lett.* 87 (2005) 241912.
- [12] M. Liu, S.W. Wang, J. Zhang, L.Q. An, L.D. Chen, *Opt. Mater.* 29 (2007) 1352.
- [13] F. Vetrone, J.C. Boyer, J.A. Capobianco, A. Speghini, M. Bettinelli, *Chem. Mater.* 15 (2003) 2737.
- [14] F. Vetrone, J.C. Boyer, J.A. Capobianco, A. Speghini, M. Bettinelli, *J. Phys. Chem. B* 107 (2003) 1107.
- [15] C.B. Zheng, Y.Q. Xia, F. Qin, Y. Yu, J.P. Miao, Z.G. Zhang, W.W. Cao, *Chem. Phys. Lett.* 496 (2010) 316.
- [16] W.W. An, J.P. Miao, Z.G. Zhang, *Chem. Phys. Lett.* 423 (2006) 386.
- [17] W.W. An, J.P. Miao, Z.G. Zhang, *Physica B* 382 (2006) 262.
- [18] W.W. An et al., *Appl. Surf. Sci.* 253 (2007) 3884.
- [19] M. Pollnau, D.R. Gamelin, S.R. Lüthi, H.U. Güdel, M.P. Hehlen, *Phys. Rev. B* 61 (2000) 3337.
- [20] D.Q. Chen, Y.S. Wang, Y.L. Yu, P. Huang, *Appl. Phys. Lett.* 91 (2007) 051920.